# Near critical phenomena in laminar boundary layers

**A. KLUWICK*, S. BRAUN* and E.A. COX+**

* *Institute of Fluid Mechanics and Heat Transfer, Vienna University of Technology, Resselgasse 3/E322, A-1040 Vienna, Austria,*
+ *School of Mathematical Sciences, University College Dublin, Belfield, Dublin 4, Ireland.*

**Abstract.** Recent developments in the construction of airfoils and rotorblades are characterized by an increasing interest in the application of so-called smart structures for active flow control. These are characterized by an interplay of sensors, actuators, real-time controlling data processing systems and the use of new materials e.g. shape alloys with the aim to increase manoeuvrability, reduce drag and radiated sound. The optimal use of such devices obviously requires a detailed insight into the flow phenomena to be controlled and in particular their sensitivity to external disturbances. In this connection locally separated boundary layer flows are of special interest. Asymptotic analysis of boundary layer separation in the limit of large Reynolds number $Re \to \infty$ has shown that in a number of cases which are of importance from a practical point of view solutions of the resulting interaction equations describing two-dimensional steady flows exist up to a limiting value $\Gamma_c$ of the relevant controlling parameter $\Gamma$ only while two branches of solutions exist in a regime $\Gamma < \Gamma_c$. The present study aims at a better understanding of near critical flows $|\Gamma - \Gamma_c| \to 0$ and in particular the changes of the flow behaviour associated with the passage of $\Gamma$ through $\Gamma_c$.

**Key words:** boundary layer theory, separation bubble, laminar-turbulent transition, Fisher's equation.

## 1. Introduction

Asymptotic analysis of high Reynolds number flows $Re \to \infty$ has shown that there exist at least two different routes leading to the formation of a separated flow region inside an otherwise attached laminar boundary layer. Firstly, the presence of an imposed adverse pressure gradient acting over a distance of order one on the typical boundary-layer length scale may cause the wall shear to decrease and finally become negative over a bounded distance before it recovers again. Examples of this so-called marginal separation are provided by the leading edge separation on slender airfoils at incidence, flow separation associated with the deflection of wall jets and flow separation in channels enforced by suction. Secondly, a firmly attached laminar boundary layer may be forced to separate due to the presence of a large adverse pressure gradient acting over a short distance caused, for example, by a surface mounted obstacle or the Kutta condition near the trailing edge of a slender airfoil.

Although these scenarios ultimately resulting in the formation of separated flow differ vastly in detail they, nevertheless, share a number of common features. Most important, it is found that a uniformly valid description of the flow behaviour close to separation requires the investigation of three layers or decks having substantially different properties. Viscosity plays a significant role inside a thin sublayer of the oncoming boundary layer (the lower deck) only while the dynamics of the flow further away from the wall is predominantely inviscid. The main portion of the boundary layer (main deck) primarily acts to transfer the displacement effects of the low speed flow inside the lower deck to the region outside the boundary layer (upper deck) and to transfer the resulting pressure response unchanged to the near wall region. While the leading order upper and main deck problems can be solved analytically, the study of the flow behaviour inside the viscous wall layer requires a numerical treatment in general. Specifically, for the 1st route it is found that the essential features of the lower deck region associated with marginally separated flows are captured by the integro-differential equation

$$\begin{aligned} A^2 - x^2 + \Gamma = -\lambda \int_{-\infty}^{x} \frac{1}{\sqrt{x-\xi}} \left[ \frac{\partial P(\xi,z,t)}{\partial \xi} + \int_{-\infty}^{\xi} \frac{\partial^2 P(\zeta,z,t)}{\partial z^2} \mathrm{d}\zeta \right] \mathrm{d}\xi \\ -\gamma \int_{-\infty}^{x} \frac{1}{(x-\xi)^{1/4}} \frac{\partial (A-h)}{\partial t} \mathrm{d}\xi - \kappa \int_{-\infty}^{x} \frac{v_w}{(x-\xi)^{1/4}} \mathrm{d}\xi \end{aligned} \tag{1}$$

where $A(x,z,t)$ and $P(x,z,t)$ denote the (negative) perturbation displacement thickness and the pressure while the parameter $\Gamma$ represents a measure of the angle of incidence, the turning angle and the suction rate, respectively. Furthermore, $x$, $z$ and $t$ denote Cartesian coordinates in the streamwise and spanwise directions and the time while $\lambda$, $\gamma$, $\kappa$ are positive constants. All quantities are suitably non-dimensionalized and scaled. Finally, $h(x,z,t)$ and $v_w(x,z,t)$ account for the effects of controlling devices such as surface mounted obstacles and suction stripes.

In contrast, if boundary layer separation is approached along route 2 then the boundary layer equations in incompressible form

$$\begin{gathered} \frac{\partial u}{\partial x} + \frac{\partial v}{\partial y} + \frac{\partial w}{\partial z} = 0\,, \\ \frac{\partial u}{\partial t} + u\frac{\partial u}{\partial x} + v\frac{\partial u}{\partial y} + w\frac{\partial u}{\partial z} = -\frac{\mathrm{d}P}{\mathrm{d}x} + \frac{\partial^2 u}{\partial y^2}\,, \\ \frac{\partial w}{\partial t} + u\frac{\partial w}{\partial x} + v\frac{\partial w}{\partial y} + w\frac{\partial w}{\partial z} = -\frac{\partial P}{\partial z} + \frac{\partial^2 w}{\partial y^2} \end{gathered} \tag{2}$$

together with the matching and boundary conditions

$$\begin{aligned} & u \to y \quad \text{for} \quad x \to -\infty\,, \\ & u \to y + A - h\,, \quad w \to \frac{B(x,z,t)}{y}\,, \quad B = -\int_{-\infty}^{x} \frac{\partial p}{\partial z} \mathrm{d}\xi \quad \text{for} \quad y \to \infty \\ & u = w = 0\,,\ v = v_w \quad \text{at} \quad y = 0 \end{aligned} \tag{3}$$

have to be solved. Here $u$, $v$, $w$ are the velocity components in $x$, $y$, $z$ directions where $y$ measures the distance from the solid wall. To close the problems (1) and (2), (3) a relationship $P = F(A)$ between $A$ and the induced pressure $P$ is required which is problem specific. Here we focus on incompressible flows where

$$P = -\frac{1}{\pi} \int_{-\infty}^{\infty} \int_{-\infty}^{\infty} \frac{\partial (A-h)(\xi,\zeta,t)/\partial \xi}{\sqrt{(x-\xi)^2 + (z-\zeta)^2}} \mathrm{d}\xi \mathrm{d}\zeta\,. \tag{4}$$

Despite the fact that the form of the interaction law $P = F(A)$ depends on the specific problem under consideration, marginally separated flows exhibit a number of properties which appear to be universal. Most important, in all known cases of marginal separation it is found that two-dimensional steady state solutions exist up to a critical value $\Gamma_c$ of $\Gamma$ only and that inside a range of values $\Gamma < \Gamma_c$ the problem is non-unique and admits two branches of solutions. As a specific example, Fig. 1 displays $A(0)$ versus $\Gamma$ for uncontrolled incompressible flow $h = v_w = 0$ past the leading edge of a slender airfoil at incidence first studied by Ruban [17] and independently by Stewartson et al. [20] where $\Gamma_c \approx 2.66$. Interestingly, similar

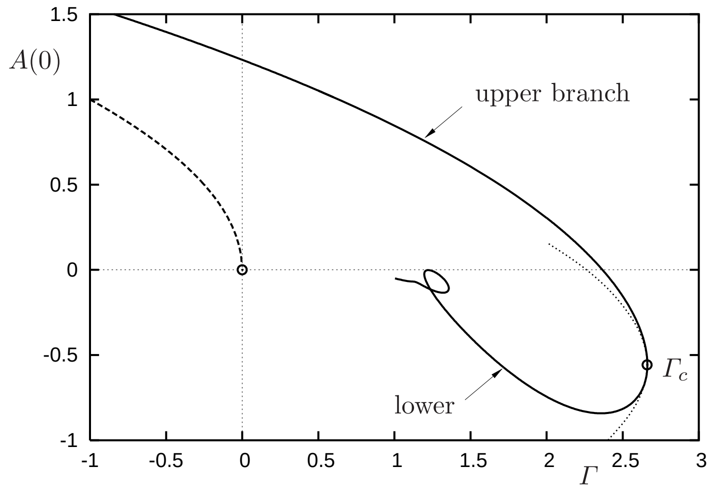


*Figure 1.* Fundamental curve of marginal separation; dashed line: local solution of classical boundary layer theory (asymptote for $\Gamma \to -\infty$), dotted line: parabola approximation near the bifurcation point, see §2.1.

phenomena are known to occur also in situations where a fully attached boundary layer separates due to rapid changes of the boundary conditions, e.g. subsonic trailing edge flow, Korolev [14], supersonic flow past flared cylinders, Gittler and Kluwick [10].

The nonexistence of steady two-dimensional solutions to equations (1) or (2), (3) supplemented with the interaction relationship $P = F(A)$ if the relevant controlling parameter exceeds a critical value raises a number of questions concerning the changes of the flow behaviour associated with its transition from sub-critical to super-critical values, e.g. Braun and Kluwick [4]. Their answer requires the investigation of unsteady, three-dimensional effects which poses an extremely difficult numerical task. To the authors knowledge it has been attacked so far for marginally separating flows only where Smith [19], Ryzhov and Smith [18], Elliott and Smith [7] noted that the evolution of unsteady two-dimensional disturbances above $\Gamma_c$ inevitably lead to the formation of finite time singularities. Probably the most detailed calculations based on the Navier–Stokes equations have been carried out by Alam and Sandham [1] for the specific case of a channel flow designed such that boundary layer separation on the lower wall is enforced by the pressure increase resulting from suction at the upper wall. The results indicate that the flow inside the separation bubble becomes increasingly sensitive to disturbances as the suction rate increases ultimately leading to bubble bursting and, if the suction rate is sufficiently high, to repeated bubble bursts in the form of self-sustained oscillations. Also, it is found that a transition from laminar to turbulent flow then occurs near and downstream of reattachment which is characterized, among others, by the formation of $\Lambda$-type vortices, Fig. 2, which is supported also by experimental evidence. Obviously, one then is confronted with the question if and how the singularities predicted by the asymptotic theories for $Re \to \infty$ are related to flow structures for large but finite Reynolds number and how much of the dynamics emerging from Navier–Stokes calculations can be captured by considering truly unsteady, three-dimensional effects described by (1) or (2), (3).

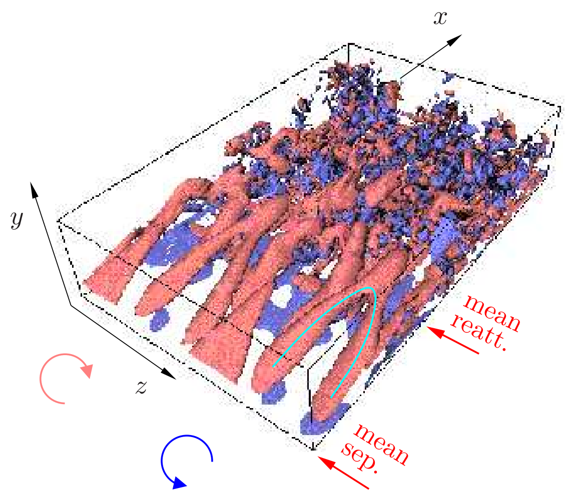


*Figure 2.* Instantaneous contours of the span-wise vorticity component $\omega_z = \partial v/\partial x - \partial u/\partial y$, [1]. $\Lambda$-vortex structures within the time mean separated region are associated with the generation of moving singularities (cyan lines) immediately after blow-up events.

## 2. Bifurcation analysis of near critical flows

### 2.1. Route 1 towards separation

As noted by Braun and Kluwick [2], [3], [4] the treatment of marginally separated flows simplifies considerably if $\Gamma$ differs only slightly from $\Gamma_c$ or, more precisely, by focussing on the limit $\varepsilon = |\Gamma - \Gamma_c|^{1/4} \to 0$. Appropriate expansions of $A, h$, and $v_w$ then are

$$\begin{aligned} A &= A_{\infty c}(x) + \varepsilon^2 a_1(x,\bar{z},\bar{t}) + \varepsilon^4 a_2(x,\bar{z},\bar{t}) + \ldots, \\ h &= h_\infty(x) + \varepsilon^4 h_1(x,\bar{z},\bar{t}) + \ldots, \\ v_w &= v_{w\infty} + \varepsilon^4 v_{w1}(x,\bar{z},\bar{t}) + \ldots \end{aligned} \tag{5}$$

Here $\bar{z} = \varepsilon z$, $\bar{t} = \varepsilon^2 t$ and the subscript '$\infty c$' refers to steady two-dimensional critical flow conditions. Introducing the abbreviations

$$I\bullet = \lambda \int_X^\infty \frac{1}{\sqrt{\xi - X}} \frac{\partial^2 \bullet}{\partial \xi^2}\, \mathrm{d}\xi\,, \quad J\bullet = \lambda \int_X^\infty \frac{\bullet\, \mathrm{d}\xi}{\sqrt{\xi - X}}\,, \quad K\bullet = \gamma \int_{-\infty}^X \frac{\bullet\, \mathrm{d}\xi}{(X-\xi)^{1/4}}\,, \tag{6}$$

substitution of expansions (5) into (1) and (4) yields $(2A_{\infty c} - I)a_1 = 0$. Consequently, $a_1 = b(x)\, c(\bar{z}, \bar{t})$ where $b(x)$ denotes the right eigenfunction of the singular operator $(2A_{\infty c} - I)$:

$$(2A_{\infty c} - I)b = 0\,. \tag{7}$$

Solutions of the equation for $a_2$

$$(2A_{\infty c} - I)a_2 = \operatorname{sgn}(\Gamma_c - \Gamma) - b^2c^2 + \frac{Jb}{2}\frac{\partial^2 c}{\partial \bar{z}^2} - Kb\frac{\partial c}{\partial \bar{t}} - Ih_1 - \frac{\kappa}{\gamma}Kv_{w1} \tag{8}$$

exist only if Fredholm's alternative is met, i.e. if the yet unknown 'shape' function $c(\bar{z}, \bar{t})$ satisfies the evolution equation

$$\frac{\partial c}{\partial \bar{t}} - \nu\frac{\partial^2 c}{\partial \bar{z}^2} + \mu c^2 - \operatorname{sgn}(\Gamma - \Gamma_c)\delta = \bar{g}\,. \tag{9}$$

The constants $\nu$, $\mu$, $\delta$ and the function $\bar{g}$ which accounts for the effects of controlling devices are uniquely defined in terms of $b(x)$ and the left eigenfunction $n(x)$: $(2A_{\infty c} - I)^* n = 0$. Here $(2A_{\infty c} - I)^*$ denotes the adjoint of $(2A_{\infty c} - I)$. Using the notation $\langle\, n, q\,\rangle = \int_{-\infty}^{\infty} nq\,\mathrm{d}x$ one obtains:

$$\nu = \frac{\langle\, n, Jb\,\rangle}{2\langle\, n, Kb\,\rangle}\,, \quad \mu = \frac{\langle\, n, b^2\,\rangle}{\langle\, n, Kb\,\rangle}\,, \quad \delta = \frac{\langle\, n, 1\,\rangle}{\langle\, n, Kb\,\rangle}\,, \quad \bar{g} = -\frac{\gamma\langle\, n, Ih_1\,\rangle + \kappa\langle\, n, Kv_{w1}\,\rangle}{\gamma\langle\, n, Kb\,\rangle}\,. \tag{10}$$

Numerical results for $A_{\infty c}(X)$, $b(x)$ and $n(x)$ with $h_\infty = v_{w\infty} = 0$ are displayed in

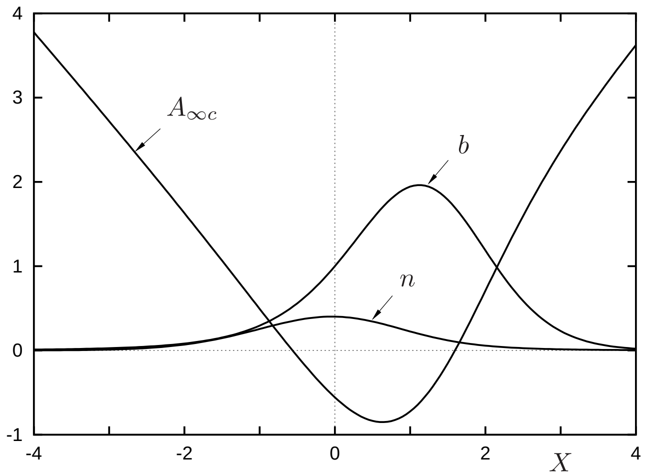


*Figure 3.* Near critical marginally separated flows ($h_\infty = v_{w\infty} = 0$): (negative) perturbation displacement thickness $A_{\infty c}(X)$, right and left eigenfunctions $b(X)$ and $n(X)$.

Fig. 3 and yield: $\nu \approx 3.0$, $\mu \approx 2.07$, $\delta \approx 1.60$. If $\Gamma < \Gamma_c$ stationary points of (9) satisfy $c = \pm c_s$, $c_s = \sqrt{\delta/\mu}$ and correspond to upper and lower branch solutions for below critical flow conditions, Fig. 1. Finally, by applying the transformation $c(\bar{z}, \bar{t}) + c_s = 2c_s\, u(z, t)$, $\bar{z} = \sqrt{\nu/(2\mu c_s)}\, z$, $\bar{t} = t/(2\mu c_s)$, $g = \bar{g}/(4\delta)$ equation (9) assumes the parameter free form

$$u_t - u_{zz} = u - u^2 - \Theta(\Gamma - \Gamma_c)/2 + g(z,t) \tag{11}$$

known as the forced Fisher-Kolmogoroff, Petrovsky, Piscounoff (FKPP)-equation, eg. Fisher [8]. Here $\Theta(s)$ denotes the Heavyside function $\Theta = 0$ for $s < 0$ and $\Theta = 1$ for $s > 0$.

### 2.2. Route 2 towards separation

The main ideas associated with the bifurcation analysis of marginally separated flows carry over unchanged although the details are considerably more complicated. To be specific, we consider the case of incompressible flow past an expansion ramp with ramp angle $\alpha$ and slightly rounded corner $h_\infty(x) = \alpha(x + \sqrt{x^2 + r^2})$, $r \ll 1$.

Generalizing equations (5) we now expand as

$$\begin{aligned}
&[u, v] = [u_{\infty c}, v_{\infty c}]\,(x, y) + \varepsilon^2\,[u_1, v_1]\,(x, y, \bar{z}, \bar{t}) + \varepsilon^4\,[u_2, v_2]\,(x, y, \bar{z}, \bar{t}) + \ldots \\
&[P, A] = [p_{\infty c}, A_{\infty c}]\,(x) + \varepsilon^2\,[P_1, A_1]\,(x, \bar{z}, \bar{t}) + \varepsilon^4\,[P_2, A_2]\,(x, \bar{z}, \bar{t}) + \ldots \\
&w = \varepsilon^3 w_1(x, y, \bar{z}, \bar{t}) + \ldots \\
&B = \varepsilon^3 B_1(x, \bar{z}, \bar{t}) + \ldots \\
&[h, v_w] = [h_\infty, v_{w\infty}]\,(x) + \varepsilon^4\,[h_2, v_{w2}]\,(x, \bar{z}, \bar{t}) + \ldots
\end{aligned} \tag{12}$$

where $\varepsilon = |\alpha - \alpha_c|^{1/4}$ and as before $\bar{z} = \varepsilon z$, $\bar{t} = \varepsilon^2 t$. Steady two-dimensional flow

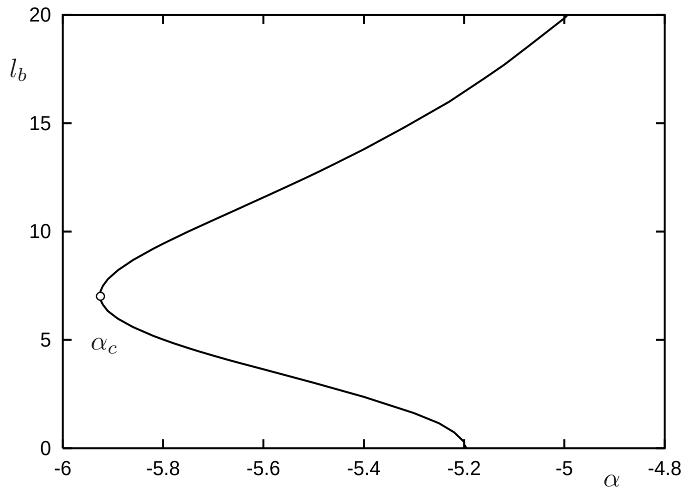


*Figure 4.* Non-uniqueness of the planar ramp flow: bubble length $l_b$ versus ramp angle $\alpha$ for $r = 0.1$ and $v_{w\infty} = 0$: $\alpha_c \approx -5.926$, source: Zametaev (2003, private communication).

fields have been computed first by Korolev [15] for $r = 0$ who found that numerical solutions cannot be obtained for $\alpha > \alpha_c$ while two branches of solutions exist for $0 \le \alpha \le \alpha_c$, Fig. 4. Similar to marginally separated flows deviations from the critical two-dimensional steady state but now characterized by the perturbations of the two velocity components $u$, $v$ and the perturbation displacement function $-A$ and expressed in terms of the vector $\vec{r}_1^{\,T} = (u_1, v_1, A_1)$ can be written as $\vec{r}_1(x, y, \bar{z}, \bar{t}) = c(\bar{z}, \bar{t})\vec{r}(x, y)$. Here $\vec{r}^{\,T}(x, y) = (u_r, v_r, A_r)$ represents the right eigenvector of a singular operator matrix $M$ which depends on the unperturbed flow quantities only:

$$M\vec{r} = \begin{pmatrix} u_c\partial_x + u_{cx} + v_c\partial_y - \partial_{yy} & u_{cy} & \frac{1}{\pi}\oint\limits_{-\infty}^{\infty} \frac{\mathrm{d}^2 \cdot /\mathrm{d}\xi^2}{x-\xi}\,\mathrm{d}\xi \\ \partial_x & \partial_y & 0 \\ 0 & 0 & \partial_y \end{pmatrix} \begin{pmatrix} u_r \\ v_r \\ A_r \end{pmatrix} = \vec{0}\,. \quad (13)$$

As before the 'shape' function $c(\bar{z}, \bar{t})$ remains arbitrary at this level of approximation and is determined by the requirement that solutions for the higher order approximations $u_2$, $v_2$, $A_2$ exist. Introducing the left eigenvector $\vec{l}^T(x, y) = (m, n, q)$ of $M$ the resulting solvability condition assumes the form

$$\begin{aligned} &\frac{\partial c}{\partial \bar{t}} \int_D m u_r \,\mathrm{d}D + c^2 \int_D m(u_r u_{rx} + v_r u_{ry})\,\mathrm{d}D + \frac{\partial^2 c}{\partial \bar{z}^2} \int\limits_D n w_r \mathrm{d}D \\ &\qquad - \mathrm{sgn}(\alpha - \alpha_c) \int_D \left( \frac{m}{\pi} \oint\limits_{-\infty}^{\infty} \frac{h_{2\xi\xi}}{x-\xi}\,\mathrm{d}\xi \right) \mathrm{d}D = \int\limits_{-\infty}^{\infty} n_0 v_{w2}\,\mathrm{d}x\,. \end{aligned} \quad (14)$$

which is again recognized as an equation of Fisher type. The quantity $w_r$ accounts for cross flow effects via the relationship $w_1 = w_r(x, y)\partial c/\partial \bar{z}$ and is obtained as the solution of

$$\begin{aligned} &u_c \frac{\partial w_r}{\partial x} + v_c \frac{\partial w_r}{\partial y} = p_r + \frac{\partial^2 w_r}{\partial y^2}\,, \\ &y = 0: \; w_r = 0\,, \quad y \to \infty: \; w_r \sim -\frac{1}{y} \int\limits_{-\infty}^{x} p_r \,\mathrm{d}\xi \quad \text{with} \quad p_r = \frac{1}{\pi} \oint\limits_{-\infty}^{\infty} \frac{A_r'}{x-\xi}\,\mathrm{d}\xi\,. \end{aligned} \quad (15)$$

Numerical work in progress (Szeywerth, private communication) indicates that the problems for the right and left eigenvectors have a unique solution and that the integrals entering (14) exist which, therefore, can transformed into its canonical form (11) which will be taken as the basis for the following discussion.

## 3. FKPP equation

Equation of Fisher's type (heat equation with nonlinear source terms) are known from nonlinear wave propagation phenomena in gene populations, reaction-diffusion and heat conduction processes. Its appearance in the context of near critical flow phenomena forms one of the key observations of the present study. In contrast to previous applications where $u(z, t)$ is limited to positive values within the range $[0, 1]$ or $[0, \infty)$ no restrictions on the magnitude and sign of $u$ exist in cases which are of interest here. As a consequence, the associated dynamics becomes considerable more complicated and only first steps towards a full understanding have been taken.

### 3.1. 2-D unsteady flows

2-D unsteady flows where further analytical progress is possible provide a natural starting point for a discussion of flow phenomena described by (11). In the case of unforced flow $\bar{g} = 0$ it reduces to Bernoulli's equation which can be solved in closed form for both sub- and super-critical flows

$$\Gamma < \Gamma_c : \quad u(t) = \frac{u_0 + u_0 \tanh[(t - t_0)/2]}{1 + (2u_0 - 1)\tanh[(t - t_0)/2]} \,, \tag{16}$$

$$\Gamma > \Gamma_c : \quad u(t) = \frac{u_0 + (u_0 - 1)\tan[(t - t_0)/2]}{1 + (2u_0 - 1)\tan[(t - t_0)/2]} \,. \tag{17}$$

Here $u_0 = u(t_0)$ denotes the value of $u$ imposed at time $t = t_0$. According to (16)

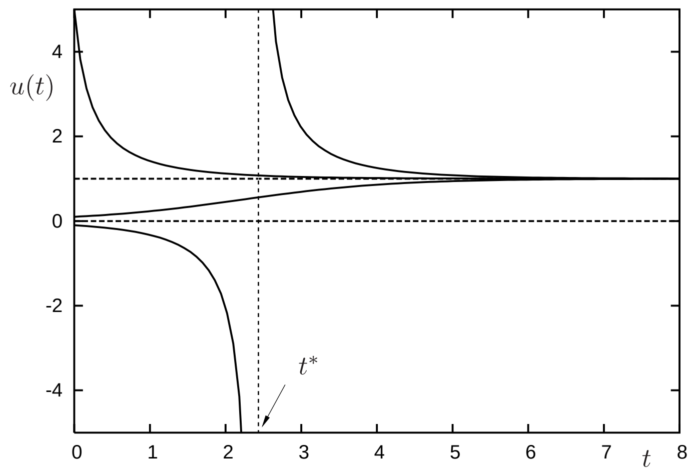


*Figure 5.* Solutions of (11) for unforced planar flow; sub-critical conditions $\Gamma < \Gamma_c$, (16); dashed lines: steady states corresponding to upper and lower branch solutions; blow-up time $t^*$.

the steady upper branch solution $u_s = 1$ is approached for initial conditions $u_0 > 0$, Fig. 5. In contrast, for $u_0 < 0$ i.e. for $u_0$ below the steady lower branch solution $u_s = 0$, finite time blow-up occurs at the blow-up time

$$t^* = t_0 + 2\,\mathrm{artanh}\left[1/(1 - 2u_0)\right] \,. \tag{18}$$

Still, however, the steady upper branch solution $u_s = 1$ is approached in the limit $t \to \infty$.

No such steady state exists for super-critical flow where equation (17) predicts periodic blow-up, i.e. self-sustained oscillations of the separation bubble.

The above interpretation of solutions to equation (11) is watertight if $u$ remains bounded for all times $t \geq t_0$ but hinges on tacit assumptions if finite time blow-up occurs, namely *(i)* that $u(t)$ can be extended beyond $t^*$ and *(ii)* that the singular behaviour of $u$ for $t - t^* \to 0^-$ causes a singular response of $u$ for $t - t^* \to 0^+$. Although no rigorous proof of *(i)* and *(ii)* exists at present, their validity appears to be supported by available numerical data and physical considerations. For example, as mentioned before, DNS calculations for marginally separated channel flows carried out by Alam and Sandham [1] predict that self-sustained bubble oscillations occur if the suction rate $\alpha = \dot{V}_s/\dot{V}_1$ where $\dot{V}_1$ and $\dot{V}_s$, respectively, denote the volume fluxes at the channel entry and the suction strip is sufficiently large. Specifically, such oscillations were observed in the range $\alpha = 0.2 \div 0.25$ which is larger than but of the same order of magnitude as the critical suction rate $\alpha_c \approx 0.09$ predicted by the asymptotic approach which is encouraging. Also, if a singular behaviour of $u(t)$ for $t-t^* \to 0^-$ is accepted, conservation of mass immediately implies a related singular behaviour for $t-t^* \to 0^+$ which in turn 'selects' unique solutions (16), (17) for arbitrary values $u_0$.

Therefore, assumptions *(i)*, *(ii)* will be adopted in the following considerations dealing with more general situations as for example unsteady 2-D forced flow where $g(t)$ is taken to be purely harmonic $g(t) = a\Theta(t)\sin\omega t$. Introduction of the transformation $u \to R$:

$$u(t) = \frac{1}{2}\left[1 + \omega\,\frac{R'(\bar{t})}{R(\bar{t})}\right], \qquad \bar{t} = \frac{\omega}{2}t - \frac{\pi}{4} \tag{19}$$

then leads to the canonical form of Mathieu's equation

$$R'' + \left[p - 2q\cos(2\bar{t})\right]R = 0 \tag{20}$$

with $p = -1/\omega^2$ and $q = 2a/\omega^2$. Taking into account (19), blow-up solutions of (11) are associated with zeros of solutions to (20) and multiple blow-up will be associated with periodic solutions of (20). For $p = a_0(q_0)$ this equation has an even $2\pi$ periodic solution with no zeros $R = c\,e_0(\bar{t};q_0)$ where $c$ is a normalization constant. Using the transformation $R = c\,e_0(\bar{t};q_0)\,\chi(\bar{t})$ application of the theorem of Leighton [16] to the resulting equation for $\chi$ shows that repetitive blow-up occurs for $\Gamma < \Gamma_c$ if the forcing amplitude $a > a_c = q_0\omega^2/2$ and is inevitable if $\Gamma > \Gamma_c$. Evaluation of the relationship $a_c = a_c(\omega)$ as displayed in Fig. 6 together with its limiting form $a_c \sim \omega/\sqrt{2}$ as $\omega \to \infty$ shows that the danger of bubble bursting in sub-critical flows decreases with increasing values of $\omega$ in agreement with experimental observations (Ruban, private communication). Numerical solutions of (11) for $\Gamma < \Gamma_c$, $\omega = 2$ and two different values of $a$ are depicted in Fig. 7 and seen to be in complete agreement with the prediction following from the analytical result $q_0 \approx 0.7268$, $a_c \approx 1.45216$.

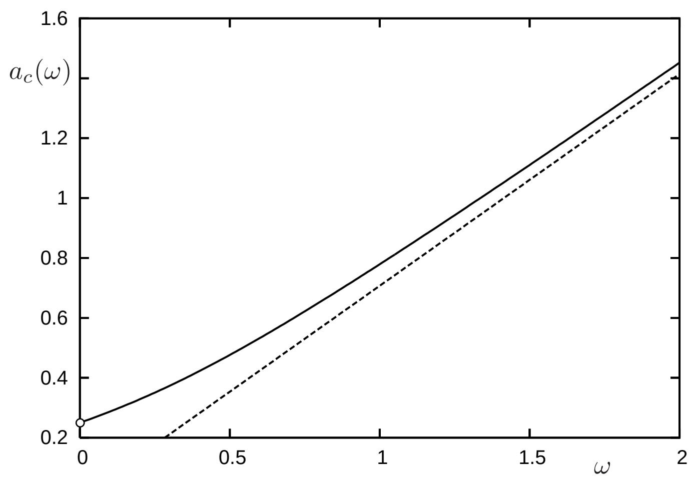


*Figure 6.* Critical forcing amplitude for planar flow and $g(t) = a\Theta(t)\sin(2t)$: $a > a_c$ leads to repetitive blow-up; $a_c(0) = 1/4$, $a_c(\omega \to \infty) \sim \omega/\sqrt{2} + \cdots$ (dashed line).

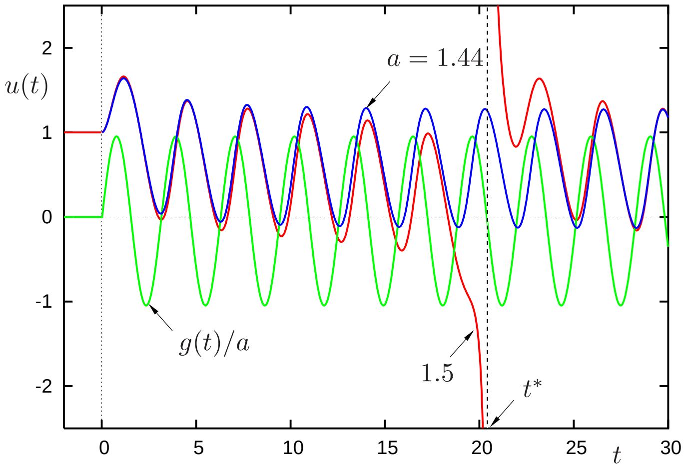


*Figure 7.* Planar forced flow: numerical solutions of (11) with $g(t) = a\Theta(t)\sin(2t)$. Repeated blow-up occurs for $a > a_c \approx 1.45216$.

## 3.2. Further analytical solutions of the FKPP equation

Closed form solutions of (11) without forcing can be obtained also in the case of steady three-dimensional flow where it reduces to the integrated form of the Korteweg-de Vries equation if $\Gamma < \Gamma_c$. Consequently, bounded solutions varying periodically with $z$ are given in terms of the Jacobian elliptic functions $\mathrm{cn}\,(s|m)$ and the integration constant $\varphi \in [0, \pi/3]$:

$$u(z) = \sin^2\left(\frac{\varphi}{2}\right) + \sqrt{3}\sin\varphi\left[\frac{1}{2} - \mathrm{cn}^2\left(\sqrt{\cos\varphi + \frac{\sin\varphi}{\sqrt{3}}}\,\frac{z}{2}\,\middle|\,\frac{2\tan\varphi}{\sqrt{3}+\tan\varphi}\right)\right] \tag{21}$$

known from the theory of shallow water waves, Fig. 8(a). The limit $\varphi = \pi/3$ yields the homoclinic orbit (solitary wave)

$$u(z) = 1 - \frac{3}{2}\cosh^{-2}\left(\frac{z}{2}\right), \tag{22}$$

while in the limit $\varphi \to 0$, which corresponds to a linearization about the unperturbed planar steady state $u = 0$, one obtains (Stokes waves)

$$u(z) \sim -\frac{\sqrt{3}}{2}\varphi\cos z + O(\varphi^2). \tag{23}$$

An additional family of solutions which vary periodically with $z$ is obtained if, as in the case of two-dimensional unsteady flow, the presence of singularities is accepted. It exists for sub-critical and, interestingly, also for super-critical flow conditions and can be expressed in terms of the Weierstrass elliptic function $\wp(z; g_2, g_3)$ with $g_2 = \mathrm{sgn}(\Gamma_c - \Gamma)/12$ while $g_3$ remains arbitrary:

$$u(z) = 6\wp(z; \mathrm{sgn}(\Gamma_c - \Gamma)/12, g_3) + 1/2. \tag{24}$$

For $\Gamma < \Gamma_c$, Fig. 8(b), the distance between consecutive singularities (streak spacing) varies between 0 and $\infty$ and a non-periodic solution is found in the limit $g_3 = -1/216$. In contrast solutions for $\Gamma > \Gamma_c$, Fig. 9, are always periodic as they

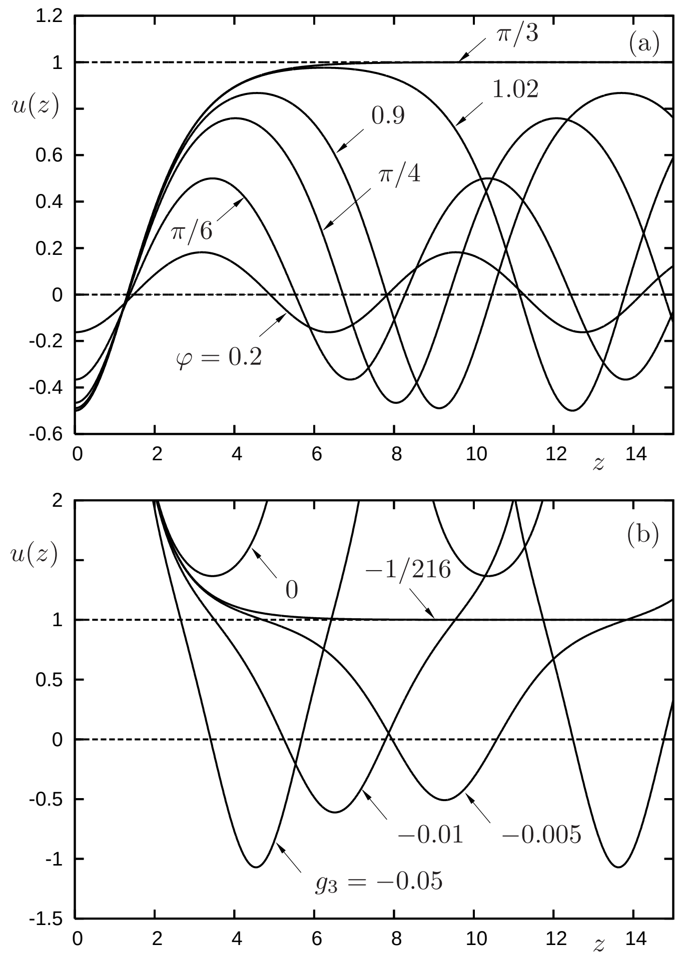


*Figure 8.* Steady sub-critical solutions of (11) without forcing; dashed lines: $u_s = 0, 1$; (a) bounded, eqns. (21), (22), (b) singular, eqn. (24).

cannot decay to a two-dimensional steady state and there exists an upper bound $\Delta z \approx 10.2909$ for the spacing of streaks.

The soliton solution (22) exhibits the exponential decay for $z \to \infty$ observed in numerical solutions for steady two-dimensional upper branch flows disturbed by an isolated three-dimensional surface mounted obstacle while the existence of periodic solutions (21) support the finding that the perturbation displacement thickness $-A$ exhibits an oscillatory behaviour for $z \to \infty$ if one considers disturbances of steady planar states corresponding to the lower branch, Braun and Kluwick [2]. The physical meaning of singular solutions (24) and in particular the possible existence of super-critical steady states associated with a maximum streak spacing remains unclear at present.

As a last class of exact solutions to the unforced version of (11) we consider travelling wave solutions

$$u(z,t) = v(\xi)\,, \quad \xi = z - Ut - \xi_0\,, \tag{25}$$

where $U$ and $\xi_0$ denote the wave speed and an arbitrary constant. For $\mathit{\Gamma} < \mathit{\Gamma}_c$ one

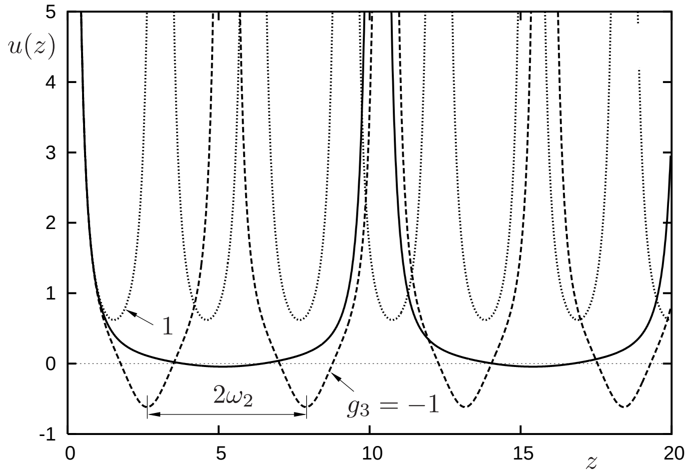


*Figure 9.* Singular steady super-critical solutions; solid line: limiting case with maximum period $2\omega_{2\max} \approx 10.2909$ ($g_3 \approx -0.00423616$).

then obtains

$$v'' + Uv' + v - v^2 = 0\,. \tag{26}$$

Because of the invariance property $u(z,t;U) = u(-z,t;-U)$ it is sufficient to consider right running waves $U > 0$ only. Except for $U = 0$ bounded solutions connect the steady states $u_s = 1, 0$, Fig. 10a. In contrast, singular travelling wave solutions are seen to deviate and return to the stable upper branch level $u = u_s = 1$, Fig. 10b.

### 3.3. Blow-up in unsteady three-dimensional flow

For two-dimensional unsteady flow the singular behaviour of $u$ near blow-up is readily obtained from the exact solution (16), (17): $u \sim 1/(t - t^*)$ as $|t - t^*| \to 0$. In the case of three-dimensional flow, however, the analysis of the flow structure is considerably more complex and a fully self-consistent description has not been obtained yet. Work carried out by Hocking et al. [11] in a different context suggests the ansatz, Braun and Kluwick [4]

$$u(z,t) \sim \frac{1}{t} f(\eta,\tau) + \cdots\,, \quad \eta = \frac{z}{\sqrt{|t|\tau}}\,, \quad \tau = -\ln|t| \tag{27}$$

as $t \to 0$ (where the blow-up point is assumed at $t^* = 0$ and $z^* = 0$ without loss of generality) and results in

$$f + \frac{\eta}{2} f_\eta - f^2 = \frac{\eta}{2\tau} f_\eta - f_\tau - \frac{\mathrm{sgn}(t)}{\tau} f_{\eta\eta} - \mathrm{sgn}(t)\,\mathrm{e}^{-\tau} f + \mathrm{e}^{-2\tau}\left[\frac{\theta(\mathit{\Gamma} - \mathit{\Gamma}_c)}{2} - g\right]. \tag{28}$$

Expansion of $f(\eta,\tau)$ for $\tau \to \infty$ requires the introduction of logarithmic terms

$$f(\eta,\tau) \sim f_0(\eta) + g_1(\eta)\frac{\ln\tau}{\tau} + \frac{f_1(\eta)}{\tau} + O\left(\frac{\ln^2\tau}{\tau^2}\right). \tag{29}$$

Near blow-up exponentially small terms in (28) can be neglected to the order considered here which in turn allows for an analytical treatment and, furthermore,

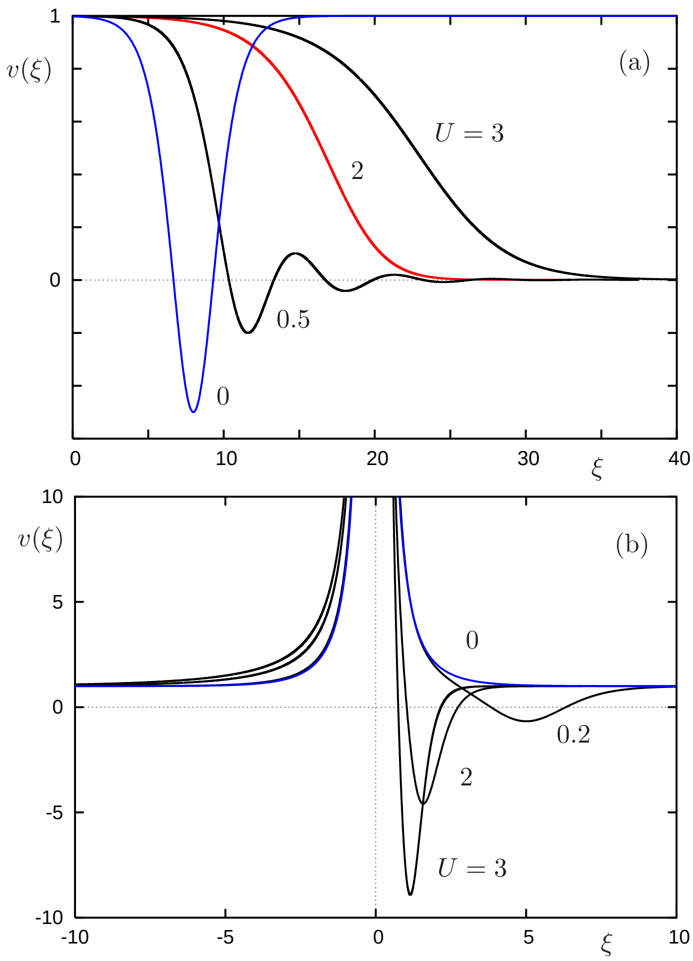


*Figure 10.* (a) bounded and (b) singular travelling (right running) wave solutions of Fisher's equation (26) depending on the wave speed $U$.

reveals the important symmetry property $f(\eta, \tau) \to f(\mathrm{i}\eta, \tau)$ if $t \to -t$ indicating that, similar to two-dimensional flows, also $z$-dependent solutions of (11) can be extended beyond blow-up and that the singular behaviour for $t \to 0^-$ forces a singular behaviour for $t \to 0^+$:

$$f_0^{\mp} = \frac{8}{8 \pm \eta^2} \,, \quad g_1^{\mp} = \mp \frac{10\,\eta^2}{(8 \pm \eta^2)^2} \,, \quad f_1^{\mp} = \frac{16 \mp c_1\eta^2 \mp 8\eta^2 \ln|8 \pm \eta^2|}{(8 \pm \eta^2)^2} \,. \tag{30}$$

Here $c_1$ is an arbitrary constant depending on initial conditions and the upper/lower sign corresponds to $t \to 0^{\mp}$. According to (30) the focussing of $u$ as the blow-up time is approached leads to the generation of a pair of vortices after blow-up moving along the paths

$$\eta_s(\tau) = \frac{z_s(t)}{\sqrt{t\tau}} = \pm\sqrt{8} + \cdots \,, \tag{31}$$

Fig. 11, which is thought to provide a mechanism for the appearance of coherent structures ($\Lambda$-vortices, see Fig. 2) in transitional separation bubbles, Braun and Kluwick [4]. Unfortunately, expansion (29) ceases to be valid in a vicinity of the moving singularities where all terms become of equal magnitude. This deficiency

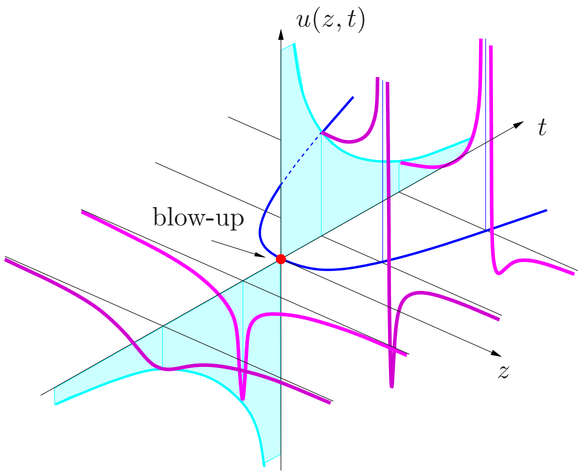


*Figure 11.* Local blow-up behaviour of solutions to Fisher's equation (11) (schematic); for $t > 0$ the solution is shown in the right half plane only.

can be partly corrected through the introduction of inner regions $(\eta \pm \sqrt{8})\tau = O(1)$ where the leading order terms represent singular travelling waves discussed in §3.2. in the limit of infinite wave speed. Higher order terms, however, cannot be matched with the outer solution (29) and, as a result, the flow description remains incomplete. Nevertheless, this analysis generalized by the method of strained coordinates indicates that $\eta_s(\tau)$ may deviate from the values $\pm\sqrt{8}$ by corrections of $O(\ln \tau/\tau)$ which appears to be supported by numerical evidence, Braun and Kluwick [4].

### 3.4. Numerical prediction of blow-up: influence of forcing

The forced FKPP equation (11) is one of many partial differential equations which have solutions that blow-up in a finite time. The blow-up typically involves the solution becoming infinite at an isolated point at a finite time. Near the blow-up point the solution develops a singular spike with both decreasing width and increasing height. To compute the solutions of blow-up accurately it is essential to employ an adaptive method which can then move points into the blow-up region. The adaptive meshing algorithm implemented here is based on the moving mesh methods of Huang, Ren and Russell [12], [13].

Defining a monitor function $M(z, t, u(z, t)) > 0$ and a computational coordinate $\xi$ an equation for the evolving mesh is given by

$$\frac{\partial}{\partial \xi}\left(M \frac{\partial z}{\partial \xi}\right) = -\sigma \frac{\partial^2}{\partial \xi^2}\left(\frac{\partial z}{\partial t}\right), \tag{32}$$

where the parameter $\sigma \ll 1$ is a relaxation time determining the time scale over which the mesh converges to a steady state. This is an approximation to the equation $Mz_\xi = 1$ modified to include temporal smoothing. The approach is to discretise (32) on a uniform $\xi$ mesh and discretise the Fisher equation using Hermite cubic collocation on the nonuniform mesh generated from (32). The choice of function $M$ is critical and motivation comes from requiring that the underlying self-similar scaling transformation exhibited by solutions of Fisher's equation near blow-up should be a property also of the numerical algorithm. In the neighbourhood of the blow-up point the linear and forcing terms in (11) are insignificant in describing the leading blow-up structure. With these terms neglected the resulting equation is invariant under the rescaling $t \to t^* + \beta(t - t^*)$, $u \to u/\beta$, $z \to z^* + \beta^{1/2}(z - z^*)$ where the blow-up point is at $(z^*, t^*)$. The choice of $M = -u$ then ensures that (32) is also invariant under these scalings near blow-up. While solutions of (11) near blow-up are not self-similar under these scalings they are approximately self similar, see (27), (29), and (30). It can be shown then, Budd, Chen, Huang and Russell [6], that for the coupled problems (11), (32) the computed mesh points near blow-up have also the desirable property of lying on trajectories for which $\eta$ given by (27) is constant. This reveals the usefulness of the moving mesh method in inheriting the natural spatial structure of the original differential equation.

An example of blow-up in finite time is shown in Fig. 12 where we see the evolution to blow-up for the applied forcing $g(z,t) = 30\sin(2t)\mathrm{e}^{-100z^2}$ with initial condition $u(z,0) = 1$. The scaling analysis above suggests that the evolution presented

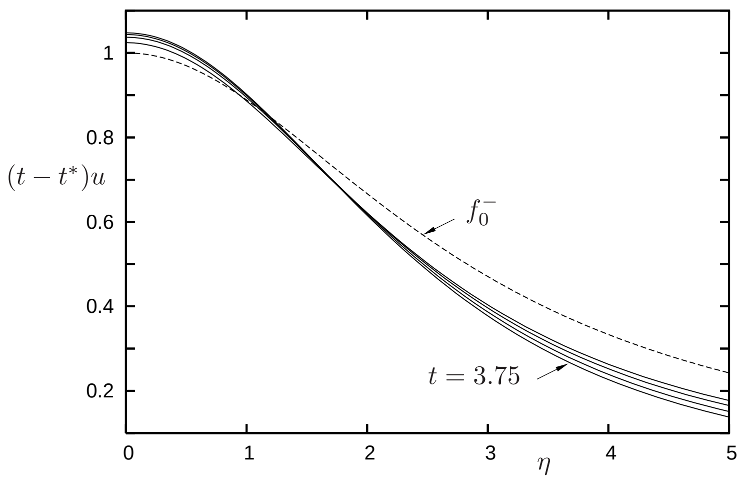


*Figure 12.* Evolution to blow-up for the applied forcing $g(z,t) = 30\sin(2t)\mathrm{e}^{-100z^2}$ with initial condition $u(z,0) = 1$. Consecutive time steps: $t = 3.75$, 3.752, 3.75349998, 3.7541998; estimated blow-up time $t^* \approx 3.75438944$, blow-up profile $f_0^-$, (30).

in Fig. 12 provides a typical structure that is independent of the precise forcing imposed in the neighbourhood of blow-up. The question is then: how are variations in the applied forcing reflected in blow-up formation? The formal asymptotics of Galaktionov, Herrero and Velázquez [9] indicate the possibility of an alternative 'flatter' asymptotic structure near blow-up described by the Hermite polynomials $H_m(y)$, $y = z/\sqrt{t^* - t}$ with $m \geq 4$ and $m$ even. We are able to generate results suggestive of this flatter blow-up structure through coalescing spike structures generated by a two-peak forcing of the form $g(z,t) = 30\sin(2t)(\mathrm{e}^{-100(z-R)^2} + \mathrm{e}^{-100(z+R)^2})$. For $R$ large there is blow-up at two points and $R$ small at one point. However for $R = R^* \approx 1.92969$ the blow-up at $z = 0$ is associated with the coalescing of two maxima. This blow-up pattern is seen in Fig. 13. More complicated and flatter blow-up patterns can also be generated by inclusion of additional peaks in the forcing and appropriate tuning of the peak separation distance.

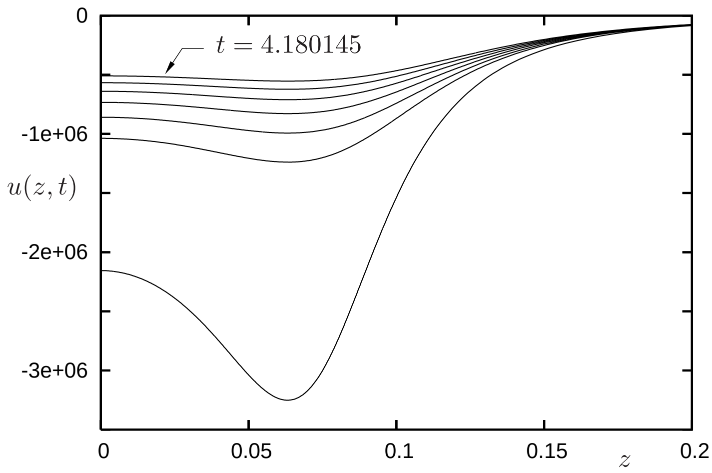


*Figure 13.* Flat blow-up structure for forcing $g(z,t) = 30\sin(2t)(\mathrm{e}^{-100(z-R)^2}+\mathrm{e}^{-100(z+R)^2})$, $R = 1.92969$ with initial conditions $u(z,0) = 1$. Consecutive time steps: $t = 4.180145 + i\Delta t$, $i = 0,2,4,6,8,10,15$; $\Delta t = 10^{-7}$.

## 4. Conclusions

In the present study it has been shown that near critical flow phenomena are governed by the same evolution equation of Fisher's type for both routes leading to the separation of high Reynolds number laminar flows analyzed in the past. Although this equation has been investigated over 70 years, the existing literature contains relatively little material which is of relevance in the present context. This is due to the fact that in most investigations carried out to date $u(z,t)$ is taken to be in the interval $[0,1]$ or $[0,\infty)$, which is sufficient if one stays within its classical field of applications, e.g. population dynamics, but is too restrictive if it is used to study near critical separated flows. Here $u$ may vary in the whole range $(-\infty,\infty)$ which significantly increases the richness of solutions. First steps towards the understanding of the associated new phenomena have been taken by Braun and Kluwick [4], [5]. Here a number of new solutions have been presented which are of interest both in the context of structure formation and flow control. For example, it has been shown that unsteady two-dimensional perturbations of a two-dimensional critical steady state caused by harmonic oscillations of a surface mounted hump starting at $t = 0$ can be expressed in terms of Mathieu functions leading in turn to a complete picture of the flow behaviour. Among others it is found that, in incompressible sub-critical flows, the critical value $a_c$ of the amplitude $a$ causing bubble bursting increases with increasing forcing frequency as observed experimentally.

In addition to analytical considerations a new numerical scheme allowing the study of general unsteady, $z$-dependent flows and specially designed to capture the phenomenon of bubble bursting in detail has been presented. Results obtained so far support existing analytical evidence that the flow properties for $|t-t^*| \to 0$ where $t^*$ denotes the bursting time are universal, i.e. independent of the specific form of the adopted forcing term but work in progress also shows that the actual value of $t^*$ is very sensitive to small changes of the forcing and thus can be controlled very effectively.

Part of this work was supported by the Austrian Science Fund FWF (project number WK W008) which is gratefully acknowledged.

## References

[1] Alam, M. & Sandham, N.D. 2000 Direct numerical simulation of ‘short’ laminar separation bubbles with turbulent reattachment. *J. Fluid Mech.* **410**, 1–28.

[2] Braun, S. & Kluwick, A. 2002 The effect of three-dimensional obstacles on marginally separated laminar boundary layer flows. *J. Fluid Mech.* **460**, 57–82.

[3] Braun, S. & Kluwick, A. 2003 Analysis of a bifurcation problem in marginally separated laminar wall jets and boundary layers. *Acta Mech.* **161**, 195–211.

[4] Braun, S. & Kluwick, A. 2004 Unsteady three-dimensional marginal separation caused by surface-mounted obstacles and/or local suction. *J. Fluid Mech.* **514**, 121–152.

[5] Braun, S. & Kluwick, A. 2005 Blow-up and control of marginally separated boundary layer flows. In *New Developments and Applications in Rapid Fluid Flows* (Eds. J.S.B. Gajjar & F.T. Smith). *Phil. Trans. R. Soc. Lond.* A **363**, 1057–1067.

[6] Budd, C.J., Chen, J., Huang, W. & Russell, R.D. 1996 Moving mesh methods with applications to blow-up problems for PDEs. In *Numerical Analysis 1995: Proceedings of 1995 Biennial Conference on Numerical Analysis* (Eds. D.F. Griffiths & G.A. Watson). Pitman Research Notes in Mathematics, Longman Scientific and Technical, pp. 1–17.

[7] Elliott, J.W. & Smith, F.T. 1987 Dynamic stall due to unsteady marginal separation. *J. Fluid Mech.* **179**, 489–512.

[8] Fisher, R.A. 1937 The wave of advance of advantageous genes. *Ann. Eugenics* **7**, 355–369.

[9] Galaktionov, V.A., Herrero M.A. & Velázquez, J.J.L. 1991 The space structure near a blow-up point for semilinear heat equations: a formal approach. *USSR Comput. Math. and Math. Physics,* **31** *(3)*, 399–411.

[10] Gittler, Ph. & Kluwick, A. 1987 Triple-deck solutions for supersonic flows past flared cylinders. *J. Fluid Mech.* **179**, 469–487.

[11] Hocking, L.M., Stewartson, K., Stuart, J.T. & Brown, S.N. 1972 A nonlinear instability burst in plane parallel flow. *J. Fluid Mech.* **51**, 705–735.

[12] Huang, W., Ren, Y. & Russell, R.D. 1994 Moving mesh methods based on moving mesh partial differential equations. *J. Comput. Phys.* **113**, 279–290.

[13] Huang, W., Ren, Y. & Russell, R.D. 1994 Moving mesh partial differential equations (MMPDEs) based upon the equidistribution principle. *SIAM J. Numer. Anal.* **31**, 709–730.

[14] Korolev, G.L. 1990 Contribution to the theory of thin-profile trailing edge separation. *Izv. Akad. Nauk SSSR: Mekh. Zhidk. Gaza* **4**, 55–59 (Engl. transl. *Fluid Dyn.* **24** *(4)*, 534–537).

[15] Korolev, G.L. 1992 Non-uniqueness of separated flow past nearly flat corners. *Izv. Akad. Nauk SSSR: Mekh. Zhidk. Gaza* **3**, 178–180 (Engl. transl. *Fluid Dyn.* **27** *(3)*, 442–444).

[16] Leighton, W. 1949 Bounds for the solutions of a second-order linear differential equation. *Proc. Natl. Acad. Sci. USA* **35**, 190–191.

[17] Ruban, A.I. 1981 Asymptotic theory of short separation regions on the leading edge of a slender airfoil. *Izv. Akad. Nauk SSSR: Mekh. Zhidk. Gaza* **1**, 42–51 (Engl. transl. *Fluid Dyn.* **17** *(1)*, 33–41).

[18] Ryzhov, O.S. & Smith, F.T. 1984 Short-length instabilities, breakdown and initial value problems in dynamic stall. *Mathematika* **31**, 163–177.

[19] Smith, F.T. 1982 Concerning dynamic stall. *Aeron. Quart.* **33**, 331–352.

[20] Stewartson, K., Smith, F.T. & Kaups, K. 1982 Marginal Separation. *Stud. in Appl. Math.* **67**, 45–61.